Tin porphyrin immobilization significantly enhances visible-light-photosensitized degradation of Microcystins: Mechanistic implications

Ha-Young Yoo [a], Shuwen Yan [b], Ji Woon Ra [c], Dahee Jeon [c], Byoungsook Goh [d], Tae-Young Kim [d], Yuri Mackeyev [e], Yong-Yoon Ahn [f], Hee-Joon Kim [g], Lon J. Wilson [e], Pedro J.J. Alvarez [h], Yunho Lee [c], Weihua Song [b], Seok Won Hong [i], Jungwon Kim [j,**], Jaesang Lee [a,f,*]

[a] Energy Environmental Policy and Technology, Green School, Korea University-KIST, Seoul 136-701, Republic of Korea
[b] Environmental Science and Engineering, Fudan University, Shanghai 200433, China
[c] Environmental Science and Engineering, Gwangju Institute of Science and Technology, Gwangju 500-712, Republic of Korea
[d] Chemistry, Gwangju Institute of Science and Technology, Gwangju 500-712, Republic of Korea
[e] Chemistry, Smalley Center for Nanoscale Science and Technology, Rice University, Houston, TX 77005, United States
[f] Civil, Environmental, and Architectural Engineering, Korea University, Seoul 136-701, Republic of Korea
[g] Applied Chemistry, Kumoh National Institute of Technology, Gumi 730-701, Republic of Korea
[h] Civil and Environmental Engineering, Rice University, Houston, TX 77005, United States
[i] Center for Water Resource Cycle Research, Korea Institute of Science and Technology, Seoul 136-791, Republic of Korea
[j] Environmental Sciences and Biotechnology, Hallym University, Chuncheon 200-702, Republic of Korea

ARTICLE INFO

ABSTRACT

This study demonstrates that tin porphyrin (SnP) loading on a silica substrate (SnP/silica) markedly accelerates the degradation of Microcystins (MCs) under visible light irradiation, despite a reduction of photosensitized singlet oxygen ($^1O_2$) production. A comparative study using Rose Bengal, SnP, and C_{60} aminofullerene suggested that the MC-RR decay rate was directly proportional to the photosensitizing activity for triplet state-induced oxidation, while it exhibited poor correlation to singlet oxygenation efficiency. This implies that electron transfer from MC to the triplet state of SnP (facilitated by favorable MC sorption on silica) contributes to the photosensitized MC oxidation. Experiments to examine sensitizers for the one-electron oxidation of 2,2′-azino-bis(3-ethylbenzothiazoline-6-sulfonic acid) showed the superiority of SnP/silica for photo-initiated electron transfer as a possible MC oxidation route. This was corroborated by the negligible effects of reagents that quench or facilitate singlet oxygenation (e.g., azide ion, D_2O) on the MC-RR degradation rate. Despite MC-RR removal below detection levels, residual toxicity (indicated by a significant decrease in protein phosphatase inhibition activity) was observed. Tandem mass spectrometric analysis suggests that this residual toxicity may be ascribed to byproducts resulting from addition of a single oxygen atom to the Adda moiety.

© 2016 Elsevier B.V. All rights reserved.

1. Introduction

An overabundance of nutrients, such as nitrogen and phosphorus, can cause population explosions of cyanobacteria in aquatic ecosystems, deteriorating water quality due to the blue-green coloration, depleted oxygen content, and production of taste-and-odor compounds [1–3]. Cyanobacterial blooms can also cause adverse biological effects as a result of their production of potent toxins that act through a broad range of toxicity mechanisms including cytotoxicity, dermal toxicity, hepatotoxicity, and neurotoxicity [4,5]. Microcystins (MCs) as a group of hepatotoxic cyclic heptapeptides constitute a dominant class of cyanobacteria-derived toxins [6], and comprise more than 80 congeners that differ in terms of amino acid composition [7]. The unique Adda (3-amino-9-methoxy-2,4,6-trimethyl-10-phenyldeca-4,6-dienoic acid) moiety, commonly found in a

majority of MC variants, enables MCs to covalently bind and inhibit protein phosphatases, serving as a key component in the biological and toxicological activity of MCs [8].

Whereas MCs undergo negligible biological, hydrolytic, and thermolytic decomposition due to their cyclic structures [9], the Adda group is susceptible to chemical oxidation by sulfate ($SO_4^{\bullet-}$) and hydroxyl ($^\bullet OH$) radicals. Attack by these radicals can lead to a significant reduction in the toxicity of MCs [10–12]. Song et al. [12] demonstrated that the addition of $^\bullet OH$ to the diene moiety of the Adda side chain initiates oxidative degradation of MC-LR (NB: a two-letter suffix of MC congeners indicates the identity and sequence of the two variant L-amino acids (e.g., leucine (L), arginine (R), tyrosine (Y), and tryptophan (W)) at the diffusion-limited rate (i.e., $k(\text{MC-LR} + ^\bullet OH) = (2.3 \pm 0.1) \times 10^{10} \, M^{-1} s^{-1}$)). Treatment of MC-LR with $SO_4^{\bullet-}$ was reported to modify the Adda group via hydroxylation of the conjugated diene bonds, which occurred in parallel with oxidation of the cyclic peptides [10]. As a result, remediation of aqueous media contaminated with MCs has been achieved using a variety of advanced oxidation processes, including UV photolysis of hydrogen peroxide and ozone [13,14], Fenton and ferrate oxidation [15,16], persulfate activation [11], and TiO_2 photocatalysis [17].

Since singlet oxygen ($^1O_2$) readily reacts with conjugated or electron-rich double bonds [18], photosensitizing agents able to produce $^1O_2$ under visible light irradiation [19,20] potentially mediate oxidative detoxification of MCs. The possible singlet oxygenation of the Adda moiety increases the likelihood that solar light induced oxidation of MCs in natural waters could be achieved with the use of humic substances to photosensitize the generation of reactive oxidizing species (ROS) (e.g., $^1O_2$ and $OH^\bullet$) [21]. Robertson et al. [22] suggested that $^1O_2$ formed by energy transfer from the photo-excited triplet state of phycocyanin (as a photosynthetic pigment of cyanobacteria) to O_2 is capable of rapidly oxidizing MC-LR. The involvement of $^1O_2$ was also confirmed based on the significant degradation of MC-LR by visible light-irradiated phthalocyanine as an effective $^1O_2$ photosensitizer [23]. In contrast, the role of $^1O_2$ in oxidative destruction of MCs was inferred to be minor by the observation that photosensitized degradation of MCs by phycocyanin was neither kinetically retarded in the presence of azide ion as a $^1O_2$ quencher nor it was negligibly accelerated in deuterated water where the lifetime of $^1O_2$ is extended [24]. The dominant pathway for photosensitized degradation of MCs in natural waters may be via direct energy transfer from the photo-excited organic matter that causes isomerization of the Adda side chain [25].

The possible photochemical transformation of MCs, either by singlet oxygenation or by direct electron transfer, suggests the applicability of visible light responsive sensitizers (catalysts) that initiate energy and electron transfer reactions for oxidative treatment of MCs in water. Our previous work [26] demonstrated that two photosensitizers, hexakis C_{60} aminofullerene (aminoC_{60}) and tin porphyrin (SnP), were capable of high yield production of $^1O_2$ and associated oxidative degradation of pharmaceutical compounds under visible light irradiation. Noteworthily, the direct electron abstraction pathway mediated by SnP (confirmed using laser flash photolysis) caused decomposition of neutral phenolic compounds (e.g., acetaminophen and amoxicillin) that were not susceptible to singlet oxygenation alone by aminoC_{60} [26]. Accordingly, exploring the link between photosensitizing activity for singlet oxygenation (or direct electron abstraction) and MC degradation efficiency is important to discern the mechanism(s) underlying the photosensitized oxidation of MCs.

In this study, we evaluated selected sensitizing agents (i.e., Rose Bengal (RB), aminoC_{60}, and SnP with high quantum yields of $^1O_2$ formation ($\Phi(^1O_2) = 0.65$–1.0 [18,27,28])) in water-soluble and immobilized forms for photochemical oxidation of MC-RR and MC-LR (chemical structures provided in Supplementary Infor-

mation, Fig. S1) in aqueous media. The capacity of sensitizers to photochemically initiate singlet oxygenation and triplet state-induced oxidation was correlated with the efficacy to decompose MCs under photo-irradiation. The photosensitized oxidation of 2,2′-azino-bis(3-ethylbenzothiazoline-6-sulfonic acid) (ABTS) by aminoC_{60}- and SnP-based sensitizers (loaded on the functionalized silica support, referred to herein as aminoC_{60}/silica and SnP/silica, respectively) was performed to probe the reaction mechanism involving direct electron transfer. The effects of various reaction conditions (e.g., $^1O_2$ quencher, electron donor, argon purging, and initial pH) on the kinetic rates of photo-induced degradation of MCs were studied to further explore the role of $^1O_2$ as the possible oxidant. The change in the residual biological activity during the photosensitized transformation of MC-RR by SnP/silica was tracked using the protein phosphatase inhibition assay, and major transformation products were identified by tandem mass spectrometry (MS/MS).

2. Materials and methods

2.1. Reagents

The chemicals that were used as-received in this study include: The chemicals that were used as received include: furfuryl alcohol (Aldrich), Rose Bengal (Aldrich), 2,2′-azino-bis(3-ethylbenzothiazoline-6-sulfonic acid) diammonium salt (Sigma), L-ascorbic acid (Sigma), sodium azide (Sigma-Aldrich), deuterium oxide (Aldrich, 99.9 at.%), Suwannee River humic acid (IHSS), protein phosphatase 2A (Millipore), 4-nitrophenyl phosphate disodium salt hexahydrate (Sigma-Aldrich), DL-dithiothreitol (Sigma-Aldrich), ethylenediaminetetraacetic acid disodium salt dehydrate (Sigma-Aldrich), protein phosphatase dilution buffer (Millipore), Tris-HCl buffer (Biosesang), sodium phosphate dibasic (Sigma-Aldrich), sodium phosphate monobasic (Sigma-Aldrich), perchloric acid (Sigma-Aldrich), sodium hydroxide (Fluka), trifluoroacetic acid (Sigma-Aldrich), methanol (Sigma-Aldrich), and phosphoric acid (Aldrich). Ultrapure deionized water ($18 \, M\Omega \, cm$) prepared with a Millipore system was used. All chemicals were of reagent grade and used without further purification or treatment.

2.2. Isolation and purification of Microcystins

Algal blooms of *Microcystis aeruginosa* were collected from the Lake Tai located in the Yangtze River delta region, East China. Extraction and purification of toxins from the natural blooms were conducted using a modification of a previously reported procedure [25], producing samples of MC-LR and MC-RR. Briefly, aqueous suspensions of cyanobacteria cells were first prepared in centrifuge tubes (placed in an ice bucket) and then were subjected to 4 cycles of 30 s sonication using an ultrasonic cell disruptor. After centrifugation at 8000 rpm for 20 min, the supernatants that remained were filtered through 0.2 μm cellulose acetate filters and stored at 4 °C. Pre-concentration of 200 mL of the resultant extracts was carried out with C-18 Sep-pack (5 g) cartridges (pre-treated sequentially with 20 mL of methanol, and 20 mL of distilled water). The samples were forced through the cartridge at a flow rate of 10 mL/min. Blockages were removed from the cartridge using an aqueous methanol solution, and MCs were finally eluted with 20 mL of methanol. The eluent fraction was concentrated to dryness using a rotary evaporator at 40 °C. Following pre-HPLC sample purification, the samples were identified by comparison with authentic standards (Sigma-Aldrich).

2.3. Preparation of sensitizers as water-soluble and immobilized forms

Water-soluble aminoC$_{60}$ was prepared via nucleophilic addition of malonic acid bis-(2-*tert*-butoxycarbonylamino-ethyl) ester (synthesized according to established procedure [29]) to double bonds of high purity C$_{60}$ (MER) through the Bingel reaction [30]. Crude hexakis adduct was isolated using a liquid chromatography, hydrolyzed and subsequently converted into its hydrochloride salt, and then purified by dialysis and dried in vacuum. *trans*-dihydroxo[5,10,15,20-tetraphenylporphyrinato]tin(IV), Sn(OH)$_2$(TPP) and *trans*-dihydroxo[5,10,15,20-tetrakis-(4-pyridyl) porphyrinato]tin(IV), Sn(OH)$_2$(TPyP) were prepared using the previously-reported method [31]. The former one (i.e., ins-SnP), which exhibits extremely low aqueous solubility, was immobilized on silica support to form tin porphyrin-based heterogeneous sensitizer, SnP/silica. The latter one was used as a starting material to produce water-soluble sensitizer, s-SnP. To enable aqueous dispersion of a SnP-based sensitizer, slow diffusion of acetone layered over aqueous 1% nitric acid solution containing Sn(OH)$_2$(TPyP) was allowed to proceed for 3 days. Filtration of the resultant solution led to production of [Sn(OH$_2$)$_2$(TPy^{H}P)](NO$_3$)$_6$ crystals as water-soluble tin porphyrin (i.e., s-SnP). Surface loading of aminoC$_{60}$ and SnP on silica-based supports were performed and the resultant products were characterized as described in our previous works [26]. AminoC$_{60}$/silica was prepared by covalently loading hexakis aminoC$_{60}$ on 3-(2-succinic anhydride)propyl functionalized silica gel via an amide-based linker. Thermogravimetric analysis (TGA: SDT Q600, TA instrument) was used to verify a weight loss of 11.2 ± 1% in temperature range of 200–420 °C (due to the thermal decomposition of organic substances on SiO$_2$) to ensure that the immobilized aminofullerene content is 0.1 mmol/g. Dehydration with silanol at 60 °C led to the immobilization of ins-SnP onto silica support. The Sn content of ca. 1.85 at.% was confirmed based on the XPS analysis of SnP/silica.

To anchor RB to 3-(2-succinic anhydride)propyl-functionalized silica gel (i.e., RB/silica) with an amide bond, introduction of an amine moiety to RB was performed as follows (Fig. S2). The reaction to yield the RB derivative (i.e., RB amine) was initiated by adding 100 mL of trimethylenediamine to 100 mL of methanol containing 10 g of RB, and the progress was controlled by TLC (thin-layer chromatography) with methanol/acetic acid (4:1) as mobile phase. After stirring at 40 °C for 36 h, the residual solid mixture was dissolved in methanol and neutralized by concentrated HCl. Separation by liquid chromatography with the silica gel column (RediSep Rf Gold® Normal-Phase, Teledyne Isco) and the subsequent solvent removal in vacuum produced RB amine as the hydrochloride salt, which was identified by the Bruker MicroTOF ESI LC–MS system (Fig. S3). Immobilization of RB amine hydrochloride was performed according to the procedure used for surface loading of aminoC$_{60}$ on the functionalized silica [26]. TGA analysis indicated a weight loss of 4% in the temperature range of 200–420 °C, which corresponds to the sensitizer loading of ca. 0.03 mmol/g (Fig. S4). RB immobilization on the silica support was confirmed using a Nicolet FT-IR spectrometer (the IR measurement was performed in ATR (attenuated total reflection mode)) (Fig. S5).

2.4. Photolytic experiments and analytical methods

Photoreactions were conducted in a magnetically-stirred cylindrical quartz reactor under air-equilibrated conditions at an ambient temperature (22 °C). Irradiation was performed with a 150-W Xe-arc lamp (Abet Technologies, LS-150) with a UV cut-off filter (λ > 400 nm) in most cases. A 4-W black light blue (BLB) lamp (Philips Co.) that covers a relatively narrow wavelength range of 350 nm–400 nm was employed to subject the experimental systems to UV-A illumination. The incident light intensity of the Xe-arc lamp and the BLB lamp was measured using a power meter (Newport 1918-R) with a silicon diode detector and a pyranometer (Apogee PYR-P) and determined to be 260.3 mW/cm^2 and 0.7 mW/cm^2, respectively. The emission spectra of the light sources, recorded using a spectropro-500 spectrophotometer (Acton Research Co.) and a spectroradiometer (Luzchem SPR-4001), are presented in Fig. S6.

The typical experimental solution (or suspension), buffered with 1 mM phosphate at pH 7.0, was prepared at an initial concentration of 50 μM water-soluble photosensitizing agent (or 0.5 g/L SnP/silica with a porphyrin content of 0.1 mmol/g; 0.5 g/L aminoC$_{60}$/silica with a fullerene content of 0.1 mmol/g). An aliquot of MC-RR (or MC-LR) stock solution (50 mg/L) was added to the solution (or suspension) to obtain a desired concentration (typically 5 mg/L). As the photochemical reaction proceeded, sample aliquots of 1 mL were withdrawn at time intervals from the photo-illuminated reactor using a 1 mL syringe, filtered through a 0.45 μm PTFE filter (Millipore), and transferred into a 2 mL amber glass vial for further analysis. The photolytic experiments were carried out at least three times for each given condition. The residual concentrations of MCs were quantified using a HPLC (Shimadzu LC-20AD) equipped with a C-18 column (ZORBAX Eclipse XDB-C18 (150 mm × 4.6 mm i.d., 5 μm)) and a UV/Vis detector set at 239 nm (SPD-20AV). The mobile phase consisted of a binary mixture of 0.05% (v/v) aqueous trifluoroacetic acid solution and methanol in the volumetric ratio of 45:55. The detection limits ranged from 0.10 to 0.15 mg/L. The kinetic rate of one-electron oxidation of ABTS was determined by spectrophotometrically monitoring the absorbance at 415 nm (Sinco co., S-3100) [32].

Mass spectrometry was performed using an Agilent 6520 quadrupole time-of-flight (Q-TOF) LC–MS/MS system equipped with electrospray ionization (ESI) source. The positive ionization mode was applied and the resulting protonated ions ([M+H$^+$]) were analyzed over an *m/z* range of 50–1200. The MS/MS analysis was used to elucidate the structure of the major products that formed as a result of photosensitized oxidation MC-RR by analyzing the tandem mass spectrum of each precursor ion. The MS/MS spectra of MC-RR were used as reference data for identifying the MS/MS fragmentation patterns of the transformation products.

2.5. Assessment of residual biological activity

A colorimetric protein phosphatase binding-inhibition assay [33] was used to assess changes in toxicity due to photosensitized oxidation of MC-RR by SnP/silica. The assay quantifies the binding affinity of MCs or their transformation products to the protein phosphatase 2A (PP2A) by measuring inhibitory effects on the PP2A activity for the dephosphorylation of *p*-nitrophenyl phosphate (*p*-NPP) (leading to the cleavage into *p*-nitrophenol (*p*-NP) and free phosphate). The conversion of *p*-NPP to *p*-NP was recorded at 405 nm with an FLx800^{TM} microplate reader (BioTek, USA). Detailed information about working solutions is available in the Supporting Information (Text S1).

In combination with quantification of the residual concentrations of MC-RR, 2-fold serial dilutions of each sample solution (obtained after photosensitized oxidation for a predetermined period of time) were carried out to prepare an eight-member dilution series for the protein phosphatase inhibition assay. All enzyme assays were performed in duplicate. 100 μL of the dilution series was transferred to the well containing 5 μL of PP2A enzyme solution in a 96-well polystyrene microtiter plate (CLS3595, Sigma Aldrich) and shaken for 10 min. After adding a 90 μL aliquot of *p*-NPP solution and incubating the plate at 37 °C for 60 min, the absorbance at 405 nm was used to monitor the formation of *p*-NP. The extent of color development inhibition (*I*) was determined

using Equation I where A denotes the absorbance measured at 405 nm, and A_{max} and A_{min} indicate the average absorbance of positive (i.e., without MC samples) and negative (i.e., without PP2A) controls.

$$I(\%) = \frac{(A_{max} - A)}{(A_{max} - A_{min})} \times 100 \qquad (I)$$

The semi-logarithmic plot of the dilution factor (n) versus I value for the corresponding diluted sample yielded the dose-response curve (Fig. S7). A four-parameter logistic model (Equation II) was used to describe the dose-response relationship. In the regression model, I_{max} and I_{min} represent the maximal and minimal extent of color development inhibition, EC_{50} is the concentration required to achieve 50% inhibition, and H denotes the Hill slope.
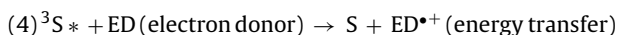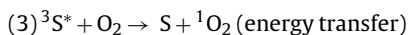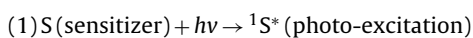
$$I(\%) = I_{min} + \frac{(I_{max} - I_{min})}{\left(1 + 10^{(\log(EC50/\left(\frac{1}{n}\right))\times H)}\right)} \qquad (II)$$

GraphPad Prism software (http://www.graphpad.com/scientific-software/prism/) was used to estimate the EC_{50} values by fitting the empirically-determined dose-response curves with the parameters including I_{max}, I_{min}, and H constrained. The toxicity of samples treated with a photosensitizing process was determined based on the potency equivalent (PEQ) value that was defined as the ratio of the EC_{50} of initial sample (containing intact MC-RR (5 μM)) to the EC_{50} of the photochemically-treated sample.

3. Results and discussion

3.1. Degradation of Microcystins by photosensitizing agents

Fig. 1a compares the rates of photochemical decomposition of furfuryl alcohol (FFA) as an indicator for $^1O_2$ production [34] by selected sensitizers including RB, s-SnP, and aminoC$_{60}$. FFA removal in the dark was not significant (data not shown) and direct photolysis in the absence of the sensitizers resulted in negligible FFA degradation (Fig. 1a). This confirms that the photosensitizing properties related to $^1O_2$ formation (Reactions 1, 2, and 3) are critical to photochemical oxidation of FFA by the aqueous systems of photosensitizers.

(1) S (sensitizer) $+ hv \rightarrow {}^1S^*$ (photo-excitation)

(2) $^1S^* \rightarrow {}^3S^*$ (intersystem crossing)

(3) $^3S^* + O_2 \rightarrow S + {}^1O_2$ (energy transfer)

(4) $^3S* + ED$ (electron donor) $\rightarrow S + ED^{\bullet+}$ (energy transfer)

Irrespective of the type of light source, the efficacy for $^1O_2$ generation ranked in the following order: RB ≈ s-SnP > aminoC$_{60}$. Visible light is superior to UV-A for the photosensitized production of $^1O_2$, which is attributable to the availability of high-intensity visible light sources and the strong visible light absorption bands of sensitizers. Since the initial FFA concentration was sufficiently low so that $^1O_2$ should be predominantly quenched by water ($k_d \gg k_r$[FFA]; k_d: rate constant for physical quenching of $^1O_2$ by water; k_r: biomolecular rate constant for singlet oxygenation of FFA), the steady-state concentration of $^1O_2$ ($[^1O_2]_{ss}$) in each photosensitizing system can be determined by the ratio of k_{exptl} to k_r (k_{exptl}: pseudo-first order rate constant for photosensitized FFA degradation) (details of the calculation of $[^1O_2]_{ss}$ is described in Supporting Information (Text S2)) [34]. $[^1O_2]_{ss}$ measured under the visible light irradiated conditions increased in the following order: RB ≈ s-SnP > aminoC$_{60}$ (Table S1).

Based on previous findings [18,22] that the Adda moiety is susceptible to $^1O_2$ attack, the photosensitizing activity to initiate singlet oxygenation was examined for degradation of MC-RR under visible light illumination (Fig. 1b). Depletion of MC-RR was not observed during direct photolysis with visible light (data not shown). Noticeable decrease in MC-RR concentration during the photo-irradiation of aqueous RB and s-SnP solutions implies a role of $^1O_2$ as an oxidant in the photosensitized MC degradation. On the other hand, MC-RR was not decomposed at all by aminoC$_{60}$ that was capable of oxidizing ca. 80% of 100 μM FFA within 10 min (Fig. 1a). Contrary to the similar rates of $^1O_2$ generation, SnP caused more rapid oxidation of MC-RR than RB, with $k = 0.0048 \pm 0.000054$ min^{-1} for SnP versus $k = 0.0020 \pm 0.000056$ min^{-1} for RB. The results reveal a relatively poor correlation between photosensitizing capacity for $^1O_2$ yield and MC-RR degradation efficiency, which suggests the possible contribution of the secondary reaction route to photochemical transformation of MCs.

In addition to singlet oxygenation, direct electron transfer involving the triplet state of a sensitizer potentially could act as an alternative reaction pathway for photochemical oxidation (Reaction 4). To identify the possible role of a triplet state in photosensitized oxidative transformation, we compared kinetic rates of degradation of 2,4,6-trimethylphenol (TMP) as a probe of the photo-excited triplet state [35] in the aqueous solutions of RB, s-SnP, and aminoC$_{60}$ (inset of Fig. 1b). TMP oxidation mediated by s-SnP proceeded 80-fold faster than by aminoC$_{60}$, and the difference in TMP decomposition rate between s-SnP and RB was also found significant, with $k = 2.375 \pm 0.1354$ min^{-1} for s-SnP versus $k = 0.4253 \pm 0.0137$ min^{-1} for RB. The observation that the highest activity of s-SnP for TMP oxidation, followed by RB and aminoC$_{60}$, led to the most effective degradation of MC-RR suggests that the higher photosensitizing capacity of s-SnP to initiate triplet-induced oxidation may be responsible for more rapid removal of MC-RR to a certain extent.

3.2. Enhanced degradation of Microcystins through SnP immobilization

SnP and aminoC$_{60}$ immobilized on silica, being readily separable for reuse [26,36], were examined for photosensitized degradation of MC-RR and MC-LR (Fig. 2a and b). Removal of MC-RR and MC-LR was minor with UV-A or visible light irradiation alone. The rapid first decay of MCs followed by a plateau was observed with SnP/silica in the dark, which implies that sorption on the silica-based host materials is likely responsible for drastic reduction in concentrations of MCs initially occurring in the visible light irradiated suspensions of the immobilized sensitizers. The fixation on silica supports led to considerable reduction in $^1O_2$ production activity compared to the corresponding homogeneous sensitizers (e.g., the pseudo first order rate constants for FFA degradation were 0.9134 ± 0.0221 min^{-1} and 0.1808 ± 0.0049 min^{-1} for s-SnP and SnP/silica, respectively) (Fig. 1a versus Fig. S8). Whereas aminoC$_{60}$/silica did not significantly decompose MCs under visible light irradiation, MCs degradation was drastically accelerated when SnP/silica was alternatively used instead of s-SnP with superior photosensitizing activity for $^1O_2$ generation (note that ca. 20-fold faster degradation of MC-RR was achievable with SnP/silica than with s-SnP) (Figs. 1b and 2b). The comparison of MC-LR degradation efficiency of RB versus RB/silica confirmed no enhancing effect via surface loading of RB sensitizer on silica support, even if RB/silica exhibited significant activity for photosensitized singlet oxygenation of FFA (Fig. S9). Also the kinetic retardation effect was not significant for photosensitized degradation of MCs by SnP/silica in the presence of an excess of FFA (i.e., 5 mM) that causes a 3- to 4-fold decrease in $[^1O_2]_{ss}$ (Text S2 in the Supporting
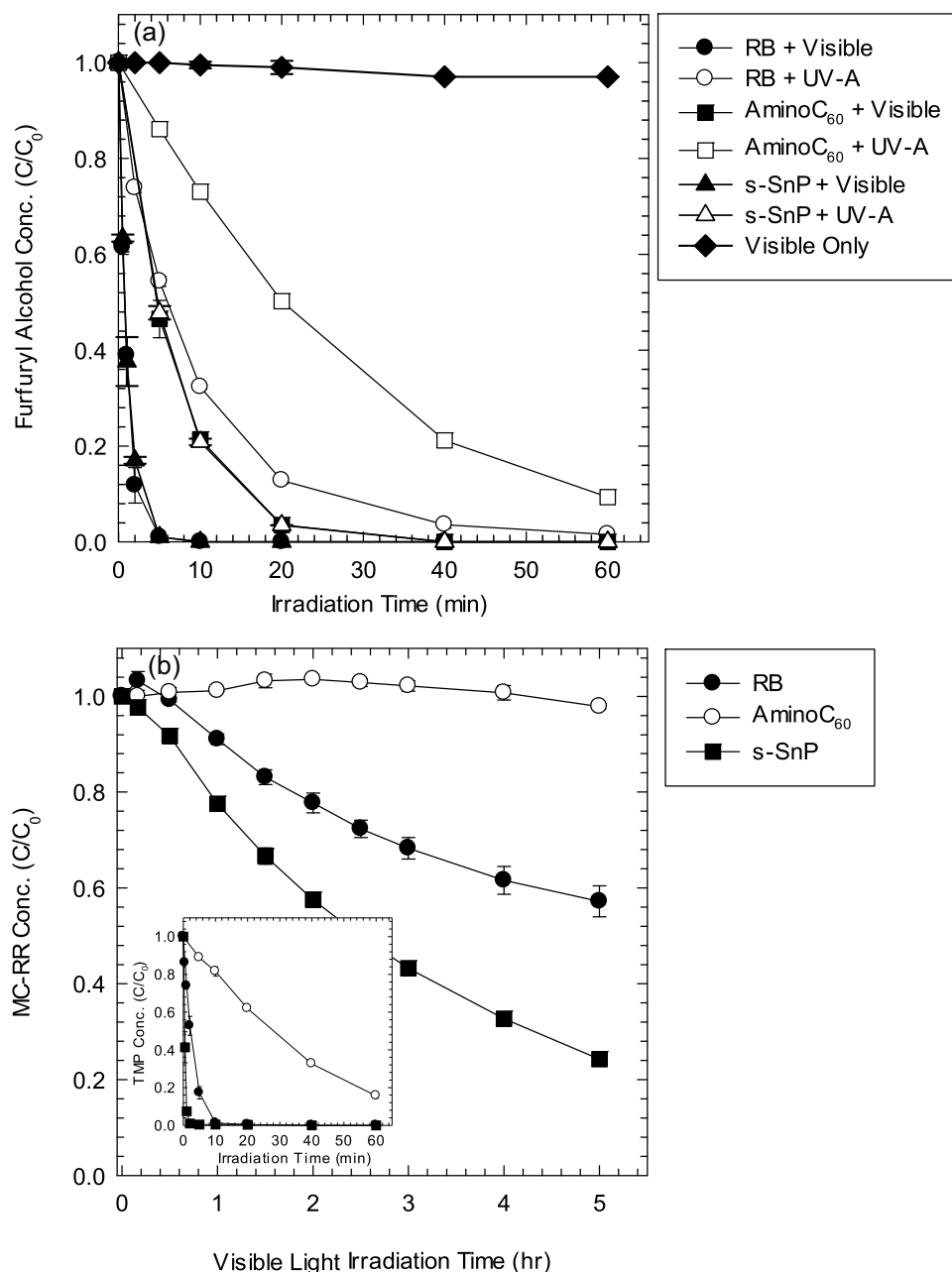
Fig. 1. Photochemical degradation of (a) furfuryl alcohol (used as a $^1O_2$ indicator) and (b) Microcystin-RR by homogeneous sensitizers (inset: photosensitized oxidation of 2,4,6-trimethylphenol under visible-light irradiation) ([RB]$_0$ = [aminoC$_{60}$]$_0$ = [s-SnP]$_0$ = 50 μM; [furfuryl alcohol]$_0$ = 100 μM; [2,4,6-trimethylphenol]$_0$ = 100 μM; [Microcystin-RR]$_0$ = 5 mg/L; [phosphate]$_0$ = 1 mM; pH$_i$ = 7.0).

Information). We found that k(MC-RR) = 0.086 ± 0.007 min^{-1} in the absence of FFA and k(MC-RR) = 0.082 ± 0.007 min^{-1} in the presence of FFA. The results imply that SnP/silica may cause the secondary MC degradation pathway that is not associated with photosensitization of $^1O_2$. The susceptibility to photosensitized oxidation by RB, aminoC$_{60}$/silica, and SnP/silica does not depend on the MC isomer type: both MC-LR and MC-RR were rapidly decomposed by SnP/silica under visible light irradiation, whereas MC isomers underwent no significant degradation in the aqueous suspensions of aminoC$_{60}$/silica. This corroborates the previous findings that the choice of MC congeners did not significantly affect the oxidative degradation kinetics and mechanisms [37,38]. Note that the primary difference between the chemical structures of MC-LR and MC-RR is only one L-amino acid (leucine versus arginine) (Fig. S1).

3.3. Photo-induced electron transfer

High-valent Sn(IV) incorporated into the porphyrin center enables electron transfer from organic substrates to ^{3}SnP* [31], providing an alternative reaction route for photocatalytic oxidative degradation. Our previous study [26] showed that visible light irradiation of SnP/silica led to rapid degradation of neutral phenolic compounds that are not susceptible to singlet oxygenation by aminoC$_{60}$/silica. It also confirmed that light intensity appeared critical, since little (if any) oxidation of phenols occurred when a low-power light source was used instead [26]. The accelerated decay of ^{3}SnP* in the presence of selected substrates as electron donors [26], monitored by laser flash photolysis, enhanced the capacity of ^{3}SnP* to accept electrons relative to the triplet states of other sensitizers (e.g., aminoC$_{60}$). Fig. 2a and b show that MCs
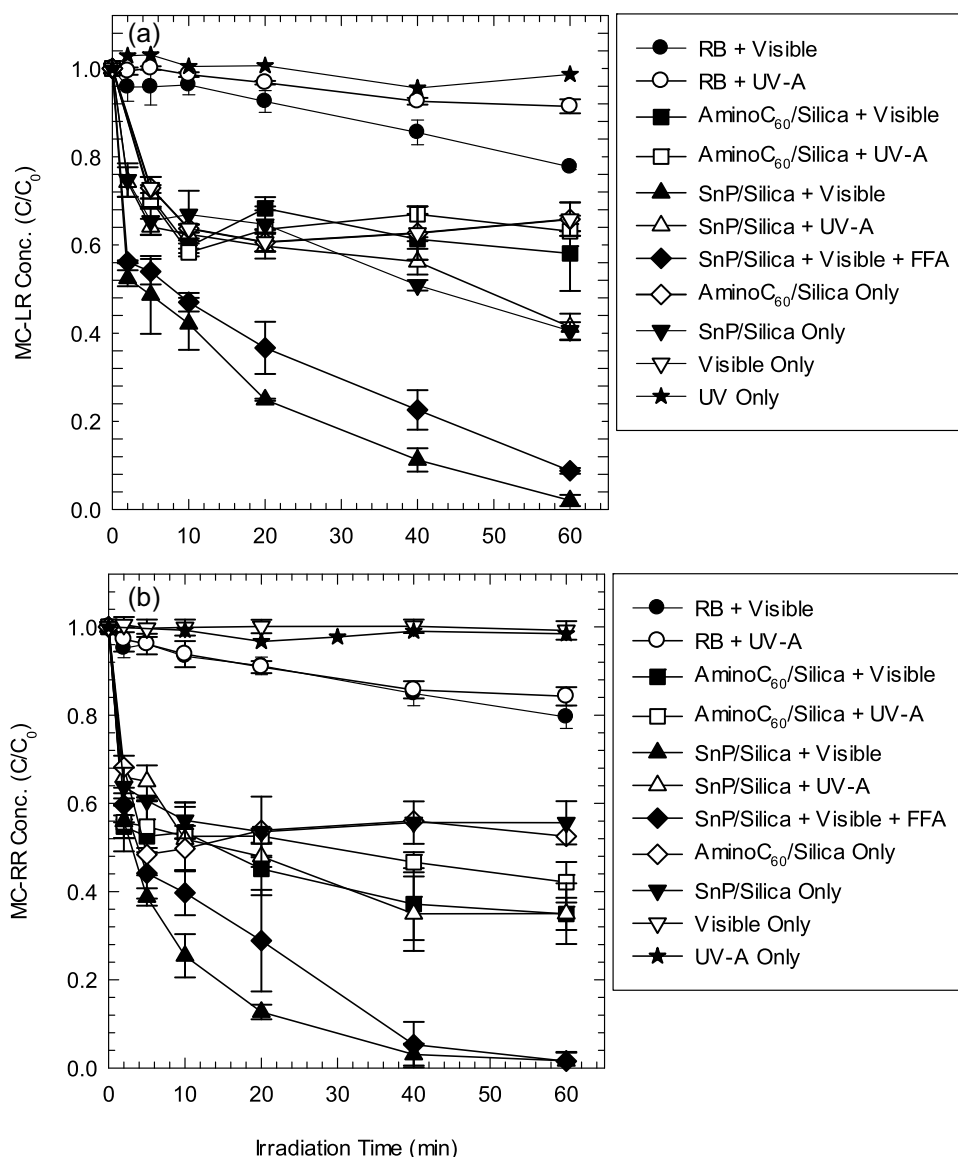
Fig. 2. Degradation of (a) Microcystin-LR and (b) Microcystin-RR by sensitizers under UV-A and visible-light irradiation ($[RB]_0 = 50\,\mu M$; $[aminoC_{60}/silica]_0 = [SnP/silica]_0 = 0.5\,g/L$; $[Microcystin-LR]_0 = [Microcystin-RR]_0 = 5\,mg/L$; $[furfuryl\ alcohol]_0 = 5\,mM$; $[phosphate]_0 = 1\,mM$; $pH_i = 7.0$).

were efficiently degraded by SnP/silica with high-intensity visible light, whereas photochemical degradation of MC was not achievable with low-power UV-A light. This result is not attributable to differences in $^1O_2$ photosensitizing efficacy because 1) no photosensitized degradation of MCs occurred with $aminoC_{60}/silica$ regardless of the applied light intensity and 2) UV-A irradiation still enabled significant production of $^1O_2$. The marked kinetic enhancement in MCs degradation suggests that photosensitized oxidation of MCs by immobilized SnP involves effective electron transfer to the excited triplet state of SnP ($^3SnP^*$), in addition to singlet oxygenation. While $^1O_2$ with a lifetime of ca. 4 microseconds [39] allows decomposition of MCs in bulk water off sensitizer surface, triplet-induced oxidation would require direct contact of MCs to the surface and subsequent electron transfer to the triplet state. Accordingly, high surface affinity of SnP/silica toward MCs (confirmed based on significant sorption of MCs) could facilitate a triplet-induced electron transfer process, leading to the pronounced acceleration in MC degradation on SnP/silica. The result is in marked contrast to insignificant kinetic enhancement in MC

decay when employing $aminoC_{60}/silica$ with relatively low activity for triplet-induced oxidation (inset of Fig. 1b).

We explored the possible photosensitized oxidation pathway involving direct electron transfer using ABTS that yields a green radical cation (ABTS•+) upon the one-electron oxidation [32]. The immobilized forms of sensitizers, including SnP/silica and $aminoC_{60}/silica$, were preferred owing to the fact that they can be separated easily and so do not interfere with spectrophotometric analysis. Fig. 3 demonstrates that a product with absorption spectrum characteristics of ABTS•+ was formed in the aqueous suspensions of SnP/silica under irradiation with high-intensity visible light, and the absorbance at 415 nm gradually increased with further photo-illumination (inset of Fig. 3). Any detectable spectral change did not occur via direct photolysis of ABTS (without SnP/silica). In particular, production of ABTS•+ was negligible when $aminoC_{60}/silica$ was alternatively applied as a photosensitizer (inset of Fig. 3). These results confirm that SnP/silica mediates the photo-initiated transfer of energy and electron concurrently, whereas singlet oxygenation (as a result of energy transfer to dissolved oxygen) is predominantly allowed with $aminoC_{60}/silica$.
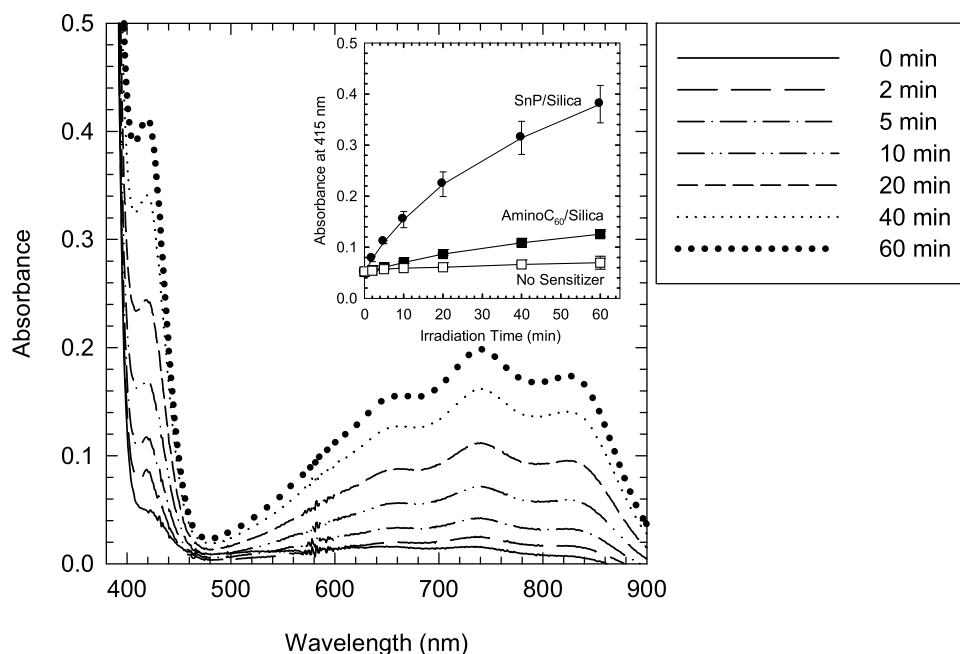
Fig. 3. Absorption spectra of ABTS in the presence of SnP/silica as a function of visible light irradiation time (inset: formation of ABTS$^{\bullet+}$ during the photo-irradiation of SnP/silica and aminoC$_{60}$/silica) ([SnP/silica]$_0$ = [aminoC$_{60}$/silica]$_0$ = 0.5 g/L; [ABTS]$_0$ = 2 mM; [phosphate]$_0$ = 1 mM; pH$_i$ = 7.0).

Accordingly, it is plausible that the capability to sensitize electron transfer is responsible for the effective decomposition of MCs by SnP/silica (Reaction 4). Energy transfer from the photo-excited triplet states of organic substances may initiate the isomerization of a diene bond in the Adda moiety [24,25,40], resulting in MC decay and formation of the corresponding product. This raises the possibility that ^{3}SnP* may be involved in this photo-induced isomerization. However, the HPLC chromatograms (Fig. S10) show that a few peaks (whose intensities increased as the photosensitized degradation proceeded) appear with elution times shorter than the peak corresponding to MC-RR. The chromatogram patterns differ from those for MC isomers that are identified as partially overlapping peaks [24], and suggest that MC removal during visible light irradiation of SnP/silica is ascribed to one-electron oxidation of MC and the subsequent conversion into degradation intermediates rather than direct energy transfer to MC and associated photosensitized isomerization.

3.4. pH effect

Fig. 4 shows that the rate of photosensitized degradation of MC-RR does not vary significantly with pH. Even though the suspension was unbuffered, pH change was minimal over the course of the photosensitized oxidation. For instance, pH varied from initial 5.12 to final 4.93 or from initial 7.06 to final 7.04 when the reaction reached completion. Sorption capacity of SnP/silica toward MC-RR changed negligibly as the pH of aqueous suspensions increased (data not shown). Since the fate of ^{3}SnP* involves energy transfer to dissolved oxygen and electron abstraction from adequate electron donors, the availability of ^{3}SnP* for photosensitized one-electron oxidation would be correlated with the efficacy of SnP/silica for the photochemical production of ^{1}O$_2$. Photosensitizing activity of SnP/silica for ^{1}O$_2$ yield was invariant with respect to the initial pH (inset of Fig. 4), which is compatible with the pH-independent kinetics of MC-RR decomposition in the visible light irradiated suspensions of SnP/silica.

3.5. Insignificant involvement of singlet oxygen

Photosensitized degradation of FFA by SnP/silica and aminoC$_{60}$/silica was kinetically enhanced in deuterated water where ^{1}O$_2$ quenching process is less effective relative to water ($k_d = 2.4 \times 10^5$ s^{-1} for H$_2$O; $k_d = 1.6 \times 10^4$ s^{-1} for D$_2$O [34]) (inset of Fig. 5a). The presence of azide ion as an ^{1}O$_2$ scavenger [34] drastically inhibited singlet oxygenation of FFA (inset of Fig. 5a). The results collectively confirm significant activity of SnP and aminoC$_{60}$ for photosensitized production of ^{1}O$_2$. On the other hand, the kinetic rate of photosensitized degradation of MC-RR by SnP/silica was not affected when deuterated water was used as a solvent, and was even accelerated to a certain extent in the presence of azide ion (Fig. 5a). Increased efficacy for MC degradation has also been observed with water-soluble phycocyanin when using azide ion as an ^{1}O$_2$ quencher [24], which excludes the possibility that SnP/silica covered with azide ions exhibits enhanced affinity toward MCs, thus improving removal efficiency. Since one-electron oxidation of azide ion leads to formation of azide radical (N$_3$$^\bullet$) as a selective oxidant (E^0(N$_3$$^\bullet$/N$_3$$^-$) = 1.3 V$_{NHE}$ [41]), this slight kinetic enhancement may be attributed to oxidative decomposition of MCs by N$_3$$^\bullet$ that likely forms via singlet oxygenation of or direct electron abstraction from azide ion by SnP/silica [42]. These reaction characteristics do not reflect the chemical reactivity of ^{1}O$_2$, and so rule out the possibility that ^{1}O$_2$ acts as the primary oxidant in the photosensitized degradation of MCs by SnP/silica. Alternatively, the addition of ascorbic acid as an electron donor, which competes with MC-RR in the photosensitized process involving electron transfer to ^{3}SnP*, drastically decreased the rate of MC-RR degradation by aqueous suspensions of SnP/silica (Fig. 5b). The retarding effect of ascorbic acid strongly implies that electron abstraction by the excited triplet state is the mechanism responsible for photochemical decomposition of MCs by organic sensitizers.

Kinetic retardation in the photosensitized degradation of MC-RR was marginal in the presence of 5 mg/L and 10 mg/L humic acid as a surrogate for natural organic matter, suggesting that triplet state-induced oxidation is not significantly quenched by back-
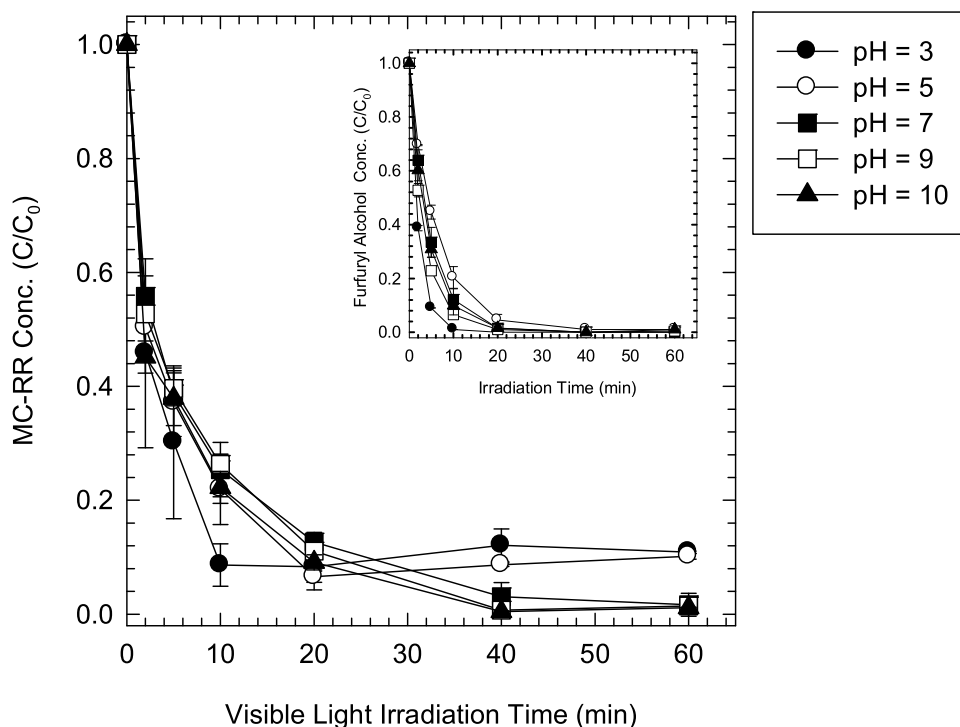
Fig. 4. Effect of initial pH on photosensitized degradation of Microcystin-RR by SnP/silica (inset: pH dependence of photosensitized singlet oxygenation) ([SnP/silica]$_0$ = 0.5 g/L; [Microcystin-RR]$_0$ = 5 mg/L; [furfuryl alcohol]$_0$ = 100 μM).

ground organic matter at environmentally-relevant concentrations (Fig. 5b). Oxidative degradation of MC-RR seems to require oxygen since residual concentrations of MC-RR after the rapid initial sorption remained constant under argon-saturated conditions. This may lead one to postulate that SnP$^{\bullet-}$ and MC$^{\bullet+}$ radicals formed via a one-electron transfer from MC to ^{3}SnP* would undergo recombination in the absence of oxygen to form the initial reactants (Reaction 5); otherwise, MC$^{\bullet+}$ reacts with oxygen to be further degraded.

$$(5)\ SnP^{\bullet-} + MC^{\bullet+} \rightarrow SnP + MC\,(recombination)$$
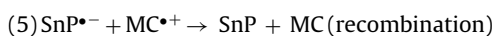
A previous study [43] also reported the hypothetic effect of O$_2$ on triplet-induced oxidation of TMP in the aqueous solution of humic substance (HS). The failure to scavenge HS$^{\bullet-}$ under deoxygenated conditions leads to the recombination with TMP$^{\bullet+}$ and subsequent regeneration of HS and TMP (i.e., HS$^{\bullet-}$ + TMP$^{\bullet+}$ → HS + TMP).

3.6. Products identification and toxic potential assessment

Several compounds were detected as major transformation products in the course of photosensitized oxidation of MC-RR by SnP/silica (Fig. 6). Their structures were identified based on MS/MS spectra of MC-RR and its oxidation products (Figs. S11-S15). The peaks at m/z = 838.4 and m/z = 878.4 represent two products resulting from cleavage of the Adda conjugated diene moiety at C4-C5 (Fig. S12) and C6-C7 (Fig. S13), respectively. The peak at m/z = 1054.6 corresponds to the two isomeric products resulting from the single addition of oxygen atom to the Adda double bond (Fig. S14). The peak at m/z = 1070.6 is related to the four isomeric products formed via the double addition of oxygen atoms to the diene bonds of the Adda group (Fig. S15). Whereas oxygen-bearing double bonds in the Adda side chain also occurred in the aqueous RB solutions, some cleavage product (at m/z = 838.4) was not detected even after 10 h of photo-illumination (data not shown). This may corroborate the involvement of different reaction pathways (i.e., singlet oxygenation versus direct electron transfer) in the photosensitized oxidation by RB and SnP/silica, though the possi-

bility that further ^{1}O$_2$ attack on the oxygenated diene structures may cause bond scission cannot be ruled out.

Fig. 7 demonstrates that the PEQ value (as a quantitative indication of relative toxicity) decreases along with the reduction in MC-RR concentration during the photosensitized oxidation by SnP/silica. This result implies that photo-initiated oxidation reaction enables the conversion of MC-RR into products with significantly lower toxic potentials. Although MC-RR was completely decomposed within 40 min, certain levels of biologically-active intermediates remained, based on the PEQ values for the samples that were subjected to further photosensitized oxidation (i.e., PEQ at 60 min = 0.11 ± 0.02). The plot of PEQ versus relative MC-RR concentration confirmed that MC-RR degradation efficiency and loss of residual toxicity are not directly proportional (inset of Fig. 7), revealing that the photosensitized oxidation of MC-RR by SnP/silica takes place predominantly, but not exclusively, via drastic structural transformation of the Adda moiety. Note that the Adda group is responsible for the non-covalent binding of MCs to protein phosphatase that leads to inhibition of the enzyme activity [33]. The toxicity that remains after the complete disappearance of MC-RR may be attributable to the reaction route involving the insertion of a single oxygen atom to the Adda diene, considering the minimal structural modification in the Adda group and no mass spectrometric evidence for oxidation of the alternative reaction sites (e.g., benzene ring of Adda amino acid) that likely undergo facile oxidative transformation. Further studies are required to probe chemical structures of the products that arise from addition of oxygen atoms to the Adda double bonds and identify the oxygen addition product that may retain enzyme inhibitory activity.

4. Conclusion

This study suggests that highly accelerated photosensitized degradation of MCs by SnP/silica is attributable to the photo-initiated electron transfer; this result appears to be in contrast to the results of previous studies [22,23,44] suggesting that the MC
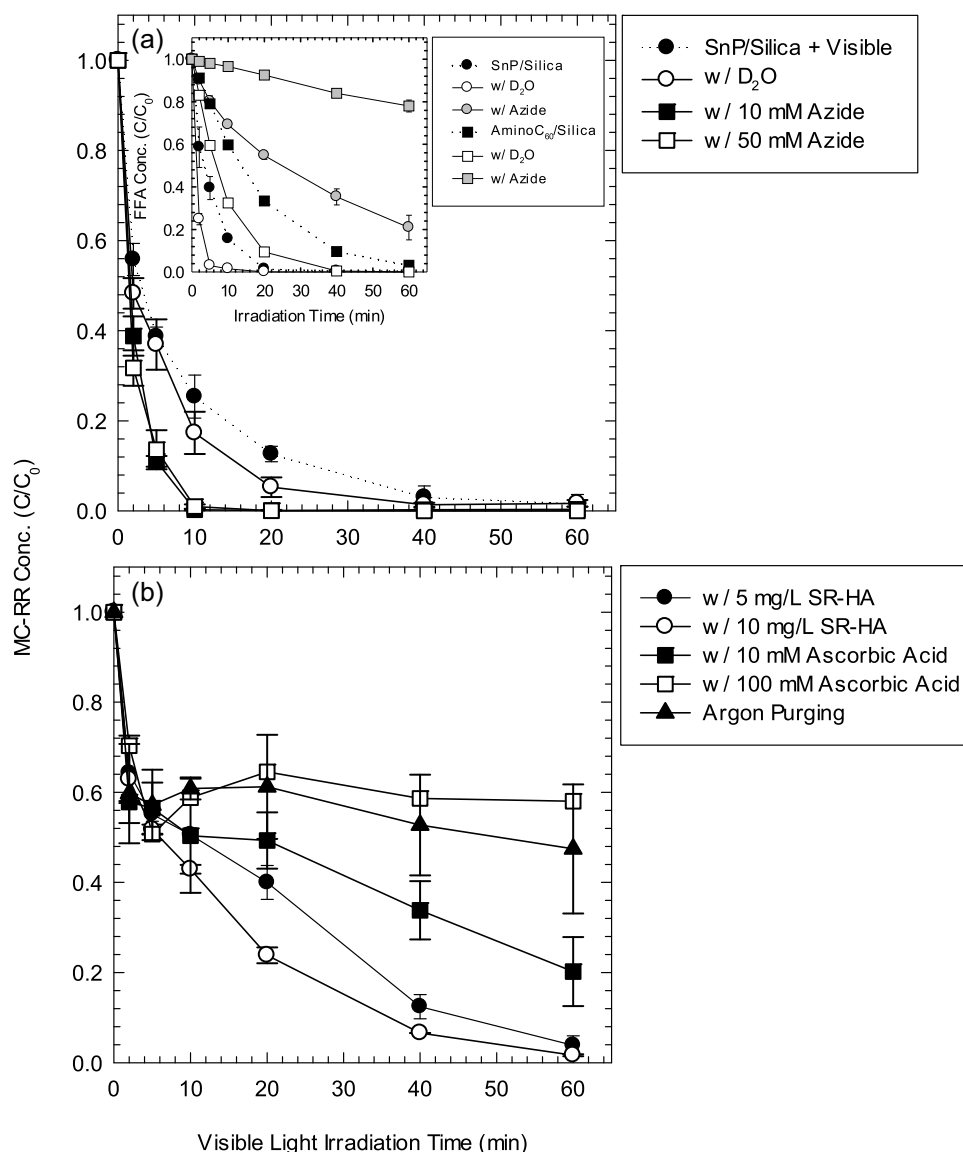
Fig. 5. (a) Photosensitized degradation of Microcystin-RR by SnP/silica in the presence of D_2O and azide ion (inset: effects of D_2O and azide ion on $^1O_2$ production); (b) variation in Microcystin-RR degradation efficiency in the absence of oxygen and in the presence of humic acid or ascorbic acid ([SnP/silica]$_0$ = [aminoC$_{60}$/silica]$_0$ = 0.5 g/L; [Microcystin-RR]$_0$ = 5 mg/L; [furfuryl alcohol]$_0$ = 100 μM; [phosphate]$_0$ = 1 mM; pH$_i$ = 7.0).

decomposition is solely associated with photosensitized energy transfer leading to $^1O_2$ production. The primary contribution of the reaction pathway involving direct electron transfer was confirmed based on (1) a stronger correlation of MC degradation rate with photosensitizing activity of triplet-induced oxidation rather than singlet oxygenation, (2) drastic kinetic enhancement in MC oxidation via SnP immobilization, and (3) kinetic dependence of photosensitized MC degradation on reaction parameters (i.e., D_2O and azide ion) affecting the lifetime of $^1O_2$ in water that is in marked contrast to kinetic dependence of FFA decomposition. In particular, a remarkable improvement in MC degradation efficiency through the immobilization of SnP offers sensitizer design strategies to achieve high performance treatment of MCs, which include (1) use of metalloporphyrins (or metallofullerenes) with the superior activity for direct electron transfer and (2) combination with host materials to enable effective MC sorption.

Dissolved organic matter (DOM) present in aquatic environment produces a variety of photo-induced reactive species including $^\bullet$OH, $^1O_2$, superoxide radical anion ($O_2^{\bullet-}$), hydrated electron (e_{aq}^-), and triplet DOM ($^3DOM^*$), and may initiate natural reduction and oxi-

dation processes [21,45,46]. The results of this study suggest that degradation of MCs in natural waters under solar light irradiation may occur via the electron transfer mechanism involving triplet states of DOMs, as photosensitized electron abstraction by humic and fulvic acids caused chemical transformation of selected substituted phenols in water [45]. With the confirmed susceptibility of MCs to triplet state-induced oxidation, the correlation between MC oxidation rate and activity of natural sensitizers for production of photo-oxidants ($^1O_2$ versus $^3DOM^*$) will be able to identify the dominant reaction pathway in the environmental fate of MCs.

The protein phosphatase inhibition assay demonstrated that SnP/silica did not sensitize the complete removal of biological activity, whereas it reduced MC-RR concentration to an undetectable level during 40 min irradiation of visible light. Among several major transformation products detected by MS/MS, the residual toxicity was ascribed mainly to the product with an additional oxygen atom attached to the Adda group. In order to further clarify the mechanisms behind the photosensitized MC degradation, it is still necessary to examine transient absorption spectroscopy to probe the quenching mechanisms of the triplet states of sensitizers (e.g.,
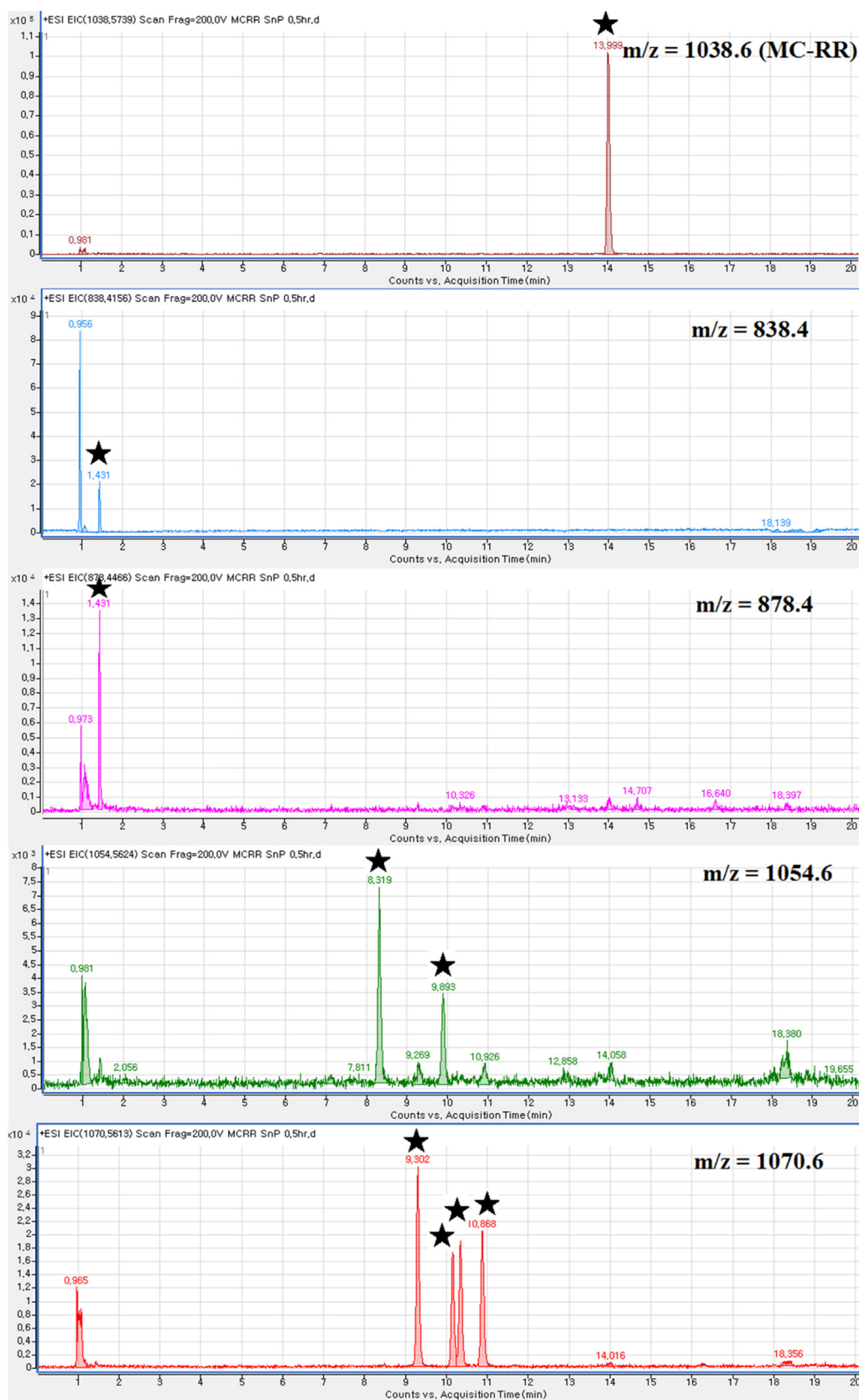
Fig. 6. LC/MS chromatograms of extracted ions of Microcystin-RR and its transformation products following treatment with SnP/silica ([SnP/silica]$_0$ = 0.5 g/L; [Microcystin-RR]$_0$ = 5 mg/L; [phosphate]$_0$ = 1 mM; pH$_i$ = 7.0, and time = 0.5 h). The peaks with stars indicate the Microcystin-RR and its transformation products whose chemical structures are proposed structures based on their MS/MS spectra (see Figs. S11–S15).
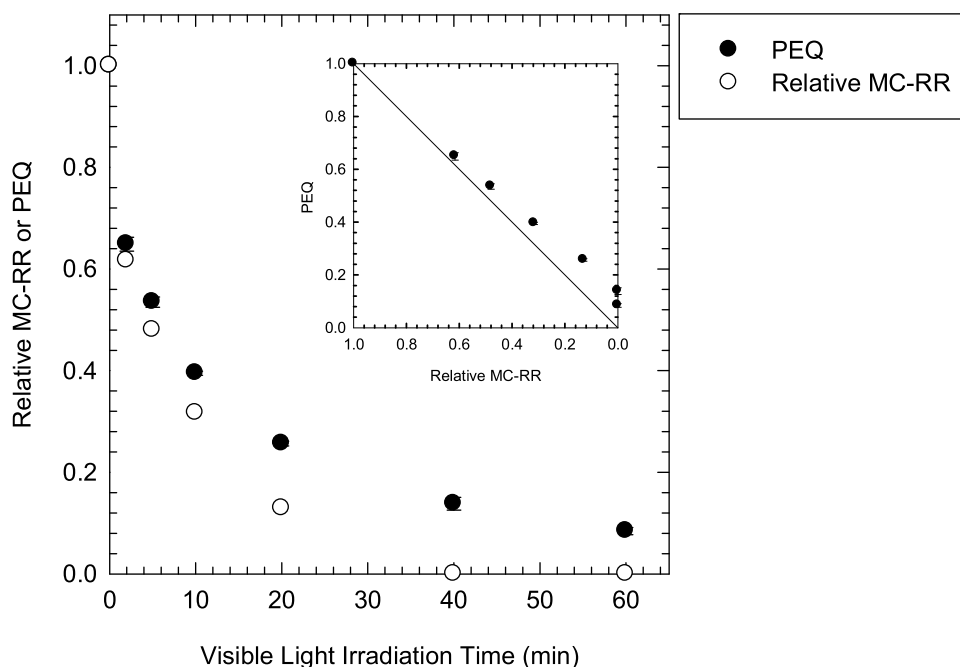
Fig. 7. Time-dependent reduction in Microcystin-RR concentration and potency equivalent (PEQ) (inset: plot of PEQ versus relative concentration of Microcystin-RR (i.e., [MC-RR]/[MC-RR]$_0$)) ([SnP/silica]$_0$ = 0.5 g/L; [Microcystin-RR]$_0$ = 5 mg/L; [phosphate]$_0$ = 1 mM; pH$_i$ = 7.0). The solid line represents a perfect negative linear correlation, which indicates that the photosensitized transformation products retain no residual toxic potential.

s-SnP and aminoC$_{60}$) in the presence of MCs, compare the spectral characteristics of short-lived intermediates formed via electron transfer versus those formed via $^1O_2$-initiated oxidation, and identify the chemical structures of the oxidation products.

Appendix A. Supplementary data

Supplementary data associated with this article can be found, in the online version, at http://dx.doi.org/10.1016/j.apcatb.2016.06.026.

References

[1] G.A. Codd, Ecol. Eng. 16 (2000) 51–60.
[2] J.L. Graham, K.A. Loftin, M.T. Meyer, A.C. Ziegler, Environ. Sci. Technol. 44 (2010) 7361–7368.
[3] G.M. Hallegraeff, Phycologia 32 (1993) 79–99.
[4] G.A. Codd, S.G. Bell, K. Kaya, C.J. Ward, K.A. Beattie, J.S. Metcalf, Eur. J. Phycol. 34 (1999) 405–415.
[5] N. Gupta, S.C. Pant, R. Vijayaraghavan, P.V.L. Rao, Toxicology 188 (2003) 285–296.
[6] B.C. Hitzfeld, S.J. Hoger, D.R. Dietrich, Environ. Health Perspect. 108 (2000) 113–122.
[7] D. Feurstein, J. Kleinteich, A.H. Heussner, K. Stemmer, D.R. Dietrich, Environ. Health Perspect. 118 (2010) 1370–1375.
[8] W.W. Carmichael, J.S. An, Nat. Toxins 7 (1999) 377–385.
[9] A.A. de la Cruz, M.G. Antoniou, A. Hiskia, M. Pelaez, W.H. Song, K.E. O'Shea, X.X. He, D.D. Dionysiou, Anti-Cancer Agents Med. Chem. 11 (2011) 19–37.
[10] M.G. Antoniou, A.A. de la Cruz, D.D. Dionysiou, Environ. Sci. Technol. 44 (2010) 7238–7244.
[11] M.G. Antoniou, A.A. de la Cruz, D.D. Dionysiou, Appl. Catal. B. Environ. 96 (2010) 290–298.
[12] W.H. Song, T.L. Xu, W.J. Cooper, D.D. Dionysiou, A.A. De La Cruz, K.E. O'Shea, Environ. Sci. Technol. 43 (2009) 1487–1492.
[13] A.M. de Freitas, C. Sirtori, C.A. Lenz, P.G.P. Zamora, Photochem. Photobiol. Sci. 12 (2013) 696–702.
[14] X.W. Liu, Z.L. Chen, N. Zhou, J.M. Shen, M.M. Ye, J. Environ. Sci. 22 (2010) 1897–1902.
[15] B.L. Yuan, J.H. Qu, M.L. Fu, Toxicon 40 (2002) 1129–1134.
[16] Y. Zhong, X.C. Jin, R.P. Qiao, X.H. Qi, Y.Y. Zhuang, J. Hazard. Mater. 167 (2009) 1114–1118.
[17] B.J.P.A. Cornish, L.A. Lawton, P.K.J. Robertson, Appl. Catal. B Environ. 25 (2000) 59–67.
[18] M.C. DeRosa, R.J. Crutchley, Coord. Chem. Rev. 233 (2002) 351–371.
[19] S.M.G. Pires, M.M.Q. Simoes, I.C.M.S. Santos, S.L.H. Rebelo, F.A.A. Paz, M.G.P.M.S. Neves, J.A.S. Cavaleiro, Appl. Catal. B Environ. 160 (2014) 80–88.
[20] P. Kluson, M. Drobek, S. Krejcikova, J. Krysa, A. Kalaji, T. Cajthaml, J. Rakusan, Appl. Catal. B Environ. 80 (2008) 321–326.
[21] M. Welker, C. Steinberg, Environ. Sci. Technol. 34 (2000) 3415–3419.
[22] P.K.J. Robertson, L.A. Lawton, B.J.P.A. Cornish, J. Porphyrins Phthalocyanines 3 (1999) 544–551.
[23] D. Jancula, L. Blahova, M. Karaskova, B. Marsalek, Water Sci. Technol. 62 (2010) 273–278.
[24] W.H. Song, S. Bardowell, K.E. O'Shea, Environ. Sci. Technol. 41 (2007) 5336–5341.
[25] S. Yan, D. Zhang, W.H. Song, Environ. Pollut. 193 (2014) 111–118.
[26] H. Kim, W. Kim, Y. Mackeyev, G.S. Lee, H.J. Kim, T. Tachikawa, S. Hong, S. Lee, J. Kim, L.J. Wilson, T. Majima, P.J.J. Alvarez, W. Choi, J. Lee, Environ. Sci. Technol. 46 (2012) 9606–9613.
[27] J.W. Arbogast, A.P. Darmanyan, C.S. Foote, Y. Rubin, F.N. Diederich, M.M. Alvarez, S.J. Anz, R.L. Whetten, J. Phys. Chem. 95 (1991) 11–12.
[28] P. Muraseccosuardi, E. Gassmann, A.M. Braun, E. Oliveros, Helv. Chim. Acta 70 (1987) 1760–1773.
[29] J. Lee, Y. Mackeyev, M. Cho, D. Li, J.H. Kim, L.J. Wilson, P.J.J. Alvarez, Environ. Sci. Technol. 43 (2009) 6604–6610.
[30] C. Bingel, Chem. Ber. 126 (1993) 1957–1959.
[31] W. Kim, J. Park, H.J. Jo, H.J. Kim, W. Choi, J. Phys. Chem. C 112 (2008) 491–499.
[32] Y. Lee, J. Yoon, U. von Gunten, Water Res. 39 (2005) 1946–1953.
[33] T. Heresztyn, B.C. Nicholson, Water Res. 35 (2001) 3049–3056.
[34] W.R. Haag, J. Hoigne, Environ. Sci. Technol. 20 (1986) 341–348.

[35] M. Minella, M.P. Merlo, V. Maurino, C. Minero, D. Vione, Chemosphere 90 (2013) 306–311.
[36] J. Lee, Y. Mackeyev, M. Cho, L.J. Wilson, J.H. Kim, P.J.J. Alvarez, Environ. Sci. Technol. 44 (2010) 9488–9495.
[37] H.F. Miao, F. Qin, G.J. Tao, W.Y. Tao, W.Q. Ruan, Chemosphere 79 (2010) 355–361.
[38] W. Song, A.A. De La Cruz, K. Rein, K.E. O'Shea, Environ. Sci. Technol. 40 (2006) 3941–3946.
[39] M.A.J. Rodgers, P.T. Snowden, J. Am. Chem. Soc. 104 (1982) 5541–5543.
[40] J.E. Grebel, J.J. Pignatello, W.A. Mitch, Water Res. 45 (2011) 6535–6544.
[41] P. Neta, R.E. Huie, A.B. Ross, J. Phys. Chem. Ref. Data 17 (1988) 1027–1284.
[42] J.R. Harbour, S.L. Issler, J. Am. Chem. Soc. 104 (1982) 903–905.
[43] S. Halladja, A. Ter Halle, J.P. Aguer, A. Boulkamh, C. Richard, Environ. Sci. Technol. 41 (2007) 6066–6073.
[44] P. Gajdek, B. Bober, E. Mej, J. Bialczyk, J. Photochem. Photobiol. B: Biol. 76 (2004) 103–106.
[45] S. Canonica, U. Jans, K. Stemmler, J. Hoigne, Environ. Sci. Technol. 29 (1995) 1822–1831.
[46] O.C. Zafiriou, J. Joussotdubien, R.G. Zepp, R.G. Zika, Environ. Sci. Technol. 18 (1984) A358–A371.